sktp-19-04-2024 07_06_36-21432

by 4 Perpustakaan UMSIDA

Submission date: 24-Apr-2024 08:09AM (UTC+0700)
Submission ID: 2359876957
File name: sktp-19-04-2024 07_06_36-214327.pdf (535.23K)
Word count: 7256
Character count: 39070

Results in Engineering 21 (2024) 101727

Contents lists available at ScienceDirect

Results in Engineering

journal homepage: www.sciencedirect.com/journal/results-in-engineering

Optimization DC-DC boost converter of BLDC motor drive by solar panel using PID and firefly algorithm

Izza Anshory [a,b,*], Jamaaluddin Jamaaluddin [a,b], Arief Wisaksono [a], Indah Sulistiyowati [a], Hindarto [c], Bagus Setya Rintyarna [d], Ahmad Fudholi [e,b,**], Yuli Asmi Rahman [f], Kamaruzzaman Sopian [g]

[a] Department of Electrical Engineering, Faculty of Science and Technology, Universitas Muhammadiyah Sidoarjo, Indonesia
[b] Research Center for Energy Conversion and Conservation, National Research and Innovation Agency (BRIN), Jakarta, Indonesia
[c] Department of Informatic Engineering, Faculty of Science and Technology, Universitas Muhammadiyah Sidoarjo, Indonesia
[d] Department of Informatic Engineering, Universitas Muhammadiyah Jember, Indonesia
[e] Solar Energy Research Institute, Universiti Kebangsaan Malaysia, Selangor, Malaysia
[f] Universitas Tadulako, Indonesia
[g] Department of Mechanical Engineering, Universiti Teknologi PETRONAS, Seri Iskandar, 32610, Perak Darul Ridzuan, Malaysia

ARTICLE INFO

Keywords:
BLDC motor
Solar panel
DC-DC boost converter
PID controller
Firefly algorithm

ABSTRACT

The use of solar photovoltaic panels as source of power for Brushless Direct Current (BLDC) motors requires a DC-DC Converter circuit. One application of solar energy is as a power source for Brushless Direct Current (BLDC) motors. The main problem is the voltage fluctuation and low DC voltage generated by the solar panel. This research aims to improve the performance of the DC-DC Boost Converter circuit and minimize voltage fluctuations. The methodology encompasses mathematical modeling of the circuit in the form of transfer functions and optimizing the DC-DC Boost Converter circuit using the Proportional Integral Derivative (PID) controller and the Firefly algorithm. Simulation testing results indicate an improvement in transient response performance of the DC-DC Converter circuit as a driver for the BLDC motor. This is evidenced by an increase in rise time from 499 s to 820 s, a decrease in settling time from 3.33 e+03 s to 2.07e+03 s, and a reduction in overshoot to 0 % from previously 11.4 %. The utilization of the firefly algorithm in optimization significantly enhances system efficiency, as demonstrated by faster achievement of stability without excessive oscillation and a reduction in the time required for the system to settle. Overall, this study shows that the firefly algorithm is effective in developing DC-DC Boost Converter circuits, improving system efficiency by reducing settling time and eliminating overshoot. These findings provide empirical evidence of the effectiveness of using artificial intelligence algorithms in enhancing the operational efficiency of energy conversion systems.

1. Introduction

The sun, as one of the renewable energy sources, has several advantages. Namely, it is the most environmentally friendly energy source, does not produce harmful emissions, and does not require additional energy in the process of generating electricity [1]. Solar energy, being a primary energy source that can reduce CO_2 emissions, the greenhouse effect, and global warming, should be utilized to generate electrical energy as a substitute for conventional fossil fuels [2]. Solar photovoltaic (PV) systems are important in generating renewable electricity to address the country electricity shortage, especially in numerous industrial electronics applications [3]. The primary goals of the PV water pumping system include minimizing costs, simplifying operations, saving energy, and enhancing dependability, with the Brushless Direct Current (BLDC) motor drive serving as a crucial component. The high-performance BLDC motor operates optimally when paired with a DC-DC Converter circuit that stabilizes the fluctuating voltage from the solar panels, ensuring efficient energy utilization and precise speed regulation [4] The high efficiency of the BLDC motor, combined with the reliability and reduced maintenance requirements of the DC-DC

* Corresponding author. Department of Electrical Engineering, Faculty of Science and Technology, Universitas Muhammadiyah Sidoarjo, Sidoarjo, Indonesia.
** Corresponding author. Solar Energy Research Institute, Universiti Kebangsaan Malaysia, Selangor, Malaysia.
E-mail addresses: izzaanshory@umsida.ac.id (I. Anshory), a.fudholi@ukm.edu.my (A. Fudholi).

https://doi.org/10.1016/j.rineng.2023.101727
Received 10 March 2023; Received in revised form 19 December 2023; Accepted 29 December 2023
Available online 30 December 2023

Converter circuit, enhances the overall effectiveness of the system [5]. This ensures prolonged operation with lower operational and maintenance costs, making it particularly well-suited for water pumping applications [6]. Due to their advantages over induction motors, such as higher efficiency, longer lifespan, increased reliability, reduced radio frequency interference and noise, and lack of maintenance, BLDC motors are frequently used in Solar Photovoltaic (SPV) system applications [7].

A DC-DC Boost Converter and a Voltage Source Inverter (VSI) are two additional components required by the Solar Photovoltaic (SPV) system to drive a Brushless Direct Current (BLDC) motor. The photovoltaic output voltage can be adjusted using the DC-DC Boost Converter before it enters the inverter. Additionally, the DC-DC Boost Converter can serve as an auxiliary tool to enable the PV generator to operate at its peak efficiency. A suitable controller is essential for optimal voltage regulation, as variations in PV temperature and solar radiation intensity frequently cause fluctuations in the generated voltage [8].

To reduce the error between the intended voltage level and the voltage at the converter output, the DC-DC Boost Converter requires a Proportional Integral Derivative (PID) controller. PID control has been utilized in previous research for voltage regulation in DC-DC Boost Converters. Employing appropriate control strategies is crucial for voltage regulation in these converters, especially given the fluctuations in input voltage and load changes. This paper provides a brief overview of previously used control strategies for boost converters, which includes the implementation of conventional Proportional-Integral-Derivative (PID) controllers, Model Predictive Control (MPC), sliding mode control, and Linear Quadratic Regulator (LQR) approaches [9]. Other researchers have indicated that the PID controller is effective in regulating motor speed and torque, particularly during changes such as motor startup or load variations. It aids in reducing speed oscillations and torque ripple, thereby enhancing motor performance. Compared to other controllers like PI and P, the PID controller also excels in reducing Total Harmonic Distortion (THD), facilitating smoother and more efficient motor operation [10].

The necessity to tune PID controllers in order to achieve the desired operating values is one of their primary drawbacks. PID controllers can be tuned using various methodologies, ranging from traditional approaches that require mathematical modeling and system response analysis to innovative techniques employing metaheuristic optimization algorithms for determining the optimal PID controller parameter values. Research on the application of metaheuristic algorithms in PV systems includes the implementation of cuckoo search optimization (CS) for Maximum Power Point Tracking (MPPT). This study compares the CS method with two other methodologies, namely the Artificial Neural Network (ANN) and Incremental Conductance (IC). The performance evaluation of the proposed CS method was conducted through a series of experiments under various operational conditions. Moreover, the tuning of the PID controller, which is critical in regulating the duty cycle of the DC-DC converter, was carried out using Particle Swarm Optimization (PSO). This step was crucial to ensure the effective implementation of the Maximum Power Point (MPP) in the system [11]. Other researchers have also investigated the use of Fractional Order PID (FOPID) controllers for DC-DC Boost converters, with parameters fine-tuned using a Genetic Algorithm (GA). The proposed FOPID controller aims to achieve superior setpoint tracking performance under load variations and parameter deviations, compared to conventional controllers. In addition, this study designs a Fractional Order Fuzzy PID controller (FFO-PID) to surpass the FOPID performance during disturbances in the control variables [12].

This research proposes utilizing PID controllers and the firefly algorithm to optimize the DC-DC Boost Converter in BLDC motor drives powered by solar panels, aiming to enhance the overall efficiency and performance of the system. The choice of the firefly algorithm in this context is motivated by its unique ability to efficiently navigate through a multitude of potential settings. It leverages a nature-inspired mechanism that mimics the movement and blinking patterns of fireflies, making it particularly effective in finding the most optimal settings for PID controllers in complex and dynamic environments.

In our research, we have developed a new mathematical model for the DC-DC Boost Converter and BLDC motor. This model helps us understand how these components interact and improve with the firefly algorithm optimization. We have also integrated this model with a PID controller to increase the system efficiency and reliability. Our study introduces a novel approach to enhancing solar-powered BLDC motors, advancing our understanding and application in this field.

The present text is organized into multiple primary sections, addressing several significant aspects of using solar energy to power BLDC motors via DC-DC Boost converters. In the first section, we delve into solar photovoltaics, elucidating the operational concepts and mathematical frameworks underlying solar cell functionality. The next section explores the DC-DC Boost Converter, including its circuit architecture and mathematical model. Following this, we focus on the mathematical modeling of brushless DC (BLDC) motors, and then on the utilization and enhancement of Proportional-Integral-Derivative (PID) controllers. Finally, we present the firefly algorithm as an innovative approach to enhancing system efficiency.

2. Method

Fig. 1 displays the block diagram for the optimization. It also illustrates the configuration developed for optimizing DC-DC Boost Converters that drive BLDC motors, using Solar Photovoltaic systems and firefly algorithms.

The primary energy source of the system, a photovoltaic panel, harnesses solar irradiance to produce Direct Current (DC), effectively transforming luminous energy into electrical energy. A Proportional-Integral-Derivative (PID) controller is utilized to regulate and enhance the efficiency of the system by adjusting outputs in real-time, ensuring a fast and consistent system response. The firefly algorithm, a metaheuristic optimization technique inspired by the natural luminescence of fireflies, plays a crucial role in improving the system performance by fine-tuning the parameters of the PID controller. To meet the voltage requirements of the system, a DC-DC Boost Converter amplifies the low DC voltage generated by the photovoltaic panel. Subsequently, a voltage source inverter converts the heightened DC voltage into the required Alternating Current (AC) to power the BLDC motor. The BLDC motor, serving as the load of the system, uses the AC from the inverter for efficient, brushless mechanical movement. This results in higher efficiency and a longer operational lifespan compared to conventional brushed DC motors.

2.1. Solar photovoltaic

Solar cells are semiconductor devices that can produce Direct Current (DC) through Photovoltaic (PV) panels by absorbing solar energy on their frontal surfaces [13]. The main component of the PV system, consisting of two or more doped silicon wafers, is the PV cell [14]. A single cell can generate only about 1 W of power, which is insufficient to meet the demands of the load. To achieve the necessary power value, a collection of solar cells is arranged in parallel and series configurations through the grid collector busbar, this assembly is referred to as a PV module. Additionally, strings of PV modules connected in series are used to attain the required voltage level [15]. A collection of strings connected in parallel forms an array to increase the output current. When not in use at night, the solar cell functions as a P–N junction diode. The equivalent circuit of the solar PV, as shown in Fig. 2, consists of a photocurrent source, a single diode model, a series resistor, and a shunt resistor.

The fundamental equations, which demonstrate the relationship between basic current interactions and the factors determining solar cell performance, are shown in Eqs. (1-2) [16], [17].

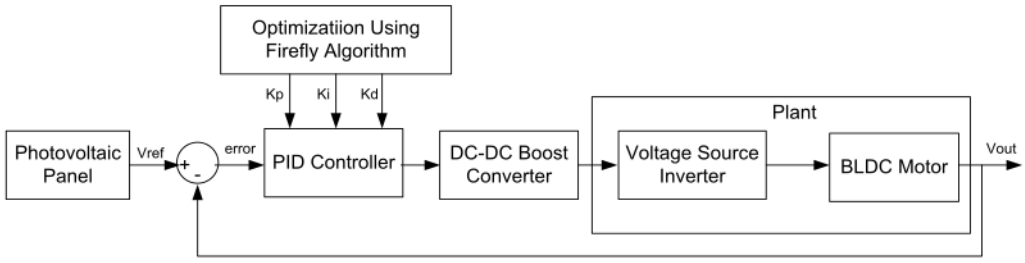

Fig. 1. Block diagram of optimization DC-DC boost converter for BLDC motor drive.

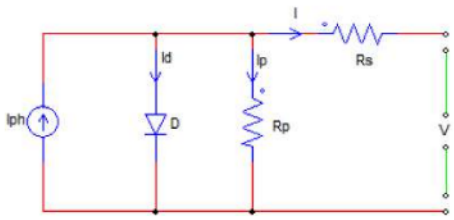

Fig. 2. Solar cell equivalent circuit.

$$I = I_{Ph} - I_d - I_p \tag{1}$$

$$I = I_{Ph} - I_0\left\{e^{\frac{q(V+R_sI}{\lambda KT}} - 1\right\} - \frac{V + R_sI}{R_p} \tag{2}$$

I is the total photovoltaic output current, I_{ph} is photocurrent, I_d is the diode current which can be represented as $I_0\left\{e^{\frac{q(V+R_sI}{\lambda KT}} - 1\right\}$. I_0 shows the diode reverse saturation current, I_p is parallel current, R_p is the parallel resistance, R_s is the series resistance, and q is the electron charge (1.6 10^{-19}C). V shows the open circuit output voltage across PV. K is Boltzmann constant (1.38 $\times$ 10^{-23} J/K).

I_{ph} can be replaced by short circuit current I_{sc}, in a short circuit state, where R_p is considered to be infinite, and the third part in the preceding equation is omitted. The analysis and optimization of performance regarding current and voltage changes in solar cells under various operational conditions are effectively elucidated in Eq. (3).

$$I = I_{SC} - I_0\left\{e^{\frac{q(V+R_sI}{\lambda KT}} - 1\right\} \tag{3}$$

The output of a PV module is influenced by several meteorological factors, including ambient temperature and uneven solar radiation. The equation that captures the relationship between the voltage in a photovoltaic (PV) cell and its internal components, while accounting for key factors such as diode voltage, current flow, and series resistance, is comprehensively presented in Eq. (4).

$$V_{PV} = V_{diode} - I_{PV}R_{series} \tag{4}$$

Parameters for the solar panels used in this study are presented in Table 1, which shows the electrical parameters of the 200 W solar panel

Table 1
Electrical parameters of the 200 W photovoltaic panel.

Maximum Power (P_m)	200 Watt
Voltage (V_{mpp})	26,01 V
Current (I_{mpp})	7,69 A
Open Circuit Voltage (V_{OC})	32,1 V
Short Circuit Current (I_{SC})	8,21 A
Total Number of Cell in Series (Ns)	54
Temperature coefficient of voltage (Tcv)	−0.07V/°C
Temperature coefficient of current (Tci)	0.002A/°C

[18].

2.2. DC-DC boost converter

A DC-DC Boost Converter is a circuit that stabilizes voltage by raising it so that the output voltage exceeds the input voltage while consuming only a modest amount of power to compensate for the voltage deficiency [19]. During the process of converting its electrical energy form, the DC-DC Boost Converter merely modifies the DC output voltage and current levels, without altering the power [20]. Fig. 3 schematically illustrates how a DC-DC Boost Converter works to convert voltage. Control is accomplished by supplying a signal or voltage that controls the switch ON and OFF periods. Pulse Width Modulation (PWM) is frequently used in the voltage signal that controls the switch.

A DC to DC converter known as a boost converter generates an output voltage that is significantly higher than the input value [21]. This Boost Converter is part of the Switched-Mode Power Supply (SMPS) circuit, which includes at least two semiconductor switches such as diodes and transistors, as well as at least one energy storage device like capacitors, inductors, or both [22]. To reduce voltage ripple, filters composed of capacitors or occasionally inductors are typically placed near the converter output.

The storage components of capacitors and inductors, as depicted in Fig. 3, are where the mathematical modeling of the DC-DC Boost Converter begins. Eqs. (5-6) provide the equations for the inductor voltage and capacitor current, respectively.

$$V_L = L\frac{di_L}{dt} \tag{5}$$

$$i_C = c\frac{dv_c}{dt}$$

The working process of the DC-DC Boost Converter begins with the switching process, resulting in two distinct circuits as shown in Figs. 4 and 5.

The mathematical equation for the DC-DC Converter in the ON position is shown in Eq. (7).

$$V_L = V_{in} \times PWM$$

The mathematical equation for the DC-DC Converter in the OFF

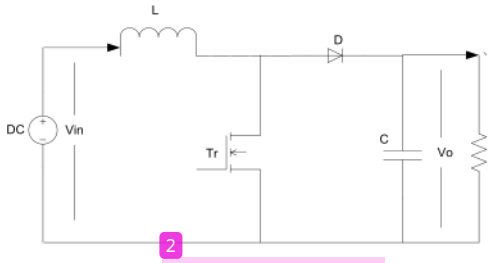

Fig. 3. DC-DC boost converter circuit.

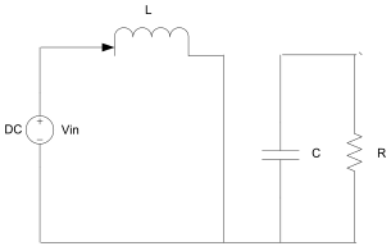

Fig. 4. DC-DC Converter ON position.

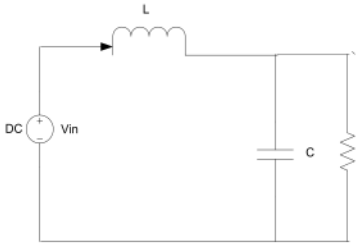

Fig. 5. DC-DC Converter OFF position.

position is shown in Eq. (8).

$$V_L = (V_{in} - V_{out}) * PWM$$

The switching process between Eqs. (7-8) is determined by the PWM switching frequency and duty cycle as shown in Eq. (9).

$$PWM = \frac{(V_0 - V_{in})}{V_0} f_{pwm}^{-1} \tag{9}$$

The current flowing through the inductor is shown in Eq. (10).

$$i_L = \frac{1}{L}\int V_L dt \tag{10}$$

The current flowing through the capacitor is shown in Eq. (11).

$$i_C = i_L - i_R \tag{11}$$

The voltage equation on the capacitor is shown in the Eq. (12).

$$V_C = \frac{1}{C}\int i_C dt \tag{12}$$

If the DC-DC Boost converter is modeled in the S-domain using the transfer function modeling technique, the total impedance functions are given by the following Eqs. 13–17.

$$Z_{total} = Z_1(s) + Z_2(s) \tag{13}$$

$$Z_1(s) = \frac{V_{in}(s)}{I(s)} = \left[R\frac{1}{C_s}\right] + L_s \tag{14}$$

$$\frac{V_{in}(s)}{I(s)} = \frac{RCLs^2 + Ls + R}{RCs + 1} \tag{15}$$

$$I(s) = \frac{RCs + 1}{RCLs^2 + Ls + R} V_{in}(s) \tag{16}$$

$$Z_2(s) = \frac{V_{out}}{I(s)} = \frac{R}{RCs + 1} \tag{17}$$

From Eqs. 16 and 17 the final equation of the transfer function for DC-DC Boost Converter is shown in Eq.(18).

$$\frac{V_{out}}{V_{in}} = \frac{R}{RCLs^2 + Ls + R} \tag{18a}$$

Table 2 shows the DC-DC Boost Converter parameters. The values used in this study are also presented [23].

2.3. Mathematical modeling of BLDC motor

The equivalent circuit of a BLDC motor, as depicted in Fig. 6, can be used to describe the configuration of the mathematical model of a BLDC motor. Resistance (R_s) and corresponding inductance serve as a representation of the stator windings for each phase (L_s). In the case of BLDC motor, the return electromotive force (EMF) per phase (e_{an}, e_{bn}, and e_{cn}) has a trapezoidal waveform, in contrast to the usual sinusoidal form [24]. The back-EMFs are separated by 120 electrical degrees. Three Hall sensors positioned inside the BLDC motor stator frame enable the three-phase inverter, which powers the motor, to quickly determine the location of the rotor magnetic field for appropriate switching [25].

The mathematical model equations for the BLDC motor circuit, as elaborately depicted in Fig. 6 are specifically outlined in Eqs. 19–21

$$V_a = I_a R_a + L\frac{di_a}{dt} + e_a \tag{19}$$

$$V_b = I_b R_b + L\frac{di_b}{dt} + e_b \tag{20}$$

$$V_c = I_c R_c + L\frac{di_c}{dt} + e_c \tag{21}$$

The mathematical equation for the mechanical time constant is shown Eq. (22).

$$\tau_m = \frac{RJ}{K_e K_t} \tag{22}$$

The equation for the electrical time constant is shown Eqs. 23 and 24.

$$\tau_e = \frac{L}{3R} \tag{23}$$

$$K_E = \frac{3RJ}{K_T \tau_M} \tag{24}$$

The transfer function equation for the BLDC motor is shown Eq. (25).

$$G(s) = \frac{\omega_m}{V_s} = \frac{1/K_e}{\tau_m \tau_e s^2 + \tau_m s + 1} \tag{25a}$$

A detailed overview of the BLDC motor parameters used in the study is shown in Table 3.

2.4. PID controller

A controller known as Proportional Integral Derivative (PID) utilizes the system feedback characteristics to assess the accuracy of an instrumentation system. The PID controller is also employed to improve dynamic response and reduce steady-state errors. The integral component of the controller minimizes steady-state error, while the derivative component improves the transient response [27]. There are three distinct types of PID control components: proportional (P), integral (I), and derivative (D), as shown in Fig. 7. Depending on the type of plant

Table 2
DC-DC boost converter parameters.

Parameter	Symbol	Value
Input Voltage	V_{in}	12 V
Inductance	L	4.7 mH
Resistance	R	100Ω
Capacitance	C	470 μF

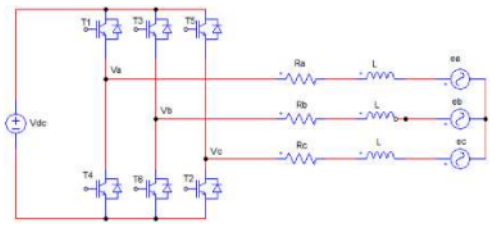

Fig. 6. BLDC motor equivalent circuit.

Table 3
BLDC motor parameters [26].

Parameters	Values	Units
Number of Poles *P*	8	–
Nominal voltage *V*	24	Volts
Terminal Resistance phase to phase *R*	1.835	Ω
Inductance L	0.287	mH
Motor Constant K_e	0.0521	V/(rad/sec)
Torque constant K_t	0.0521	Kg m/A
PM rotor inertia *J*	19×10^{-6}	Kg•m^2

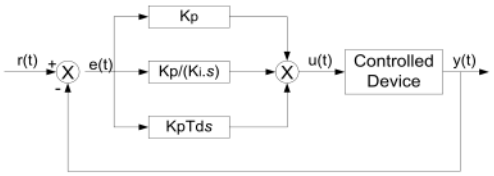

Fig. 7. Block diagram of PID controller.

and the required response, all three components can be used concurrently or individually [28].

The transfer function of the PID controller is represented by the following equation, as detailed in Eqs 26 and 27.

$$k_p + \frac{k_i}{s} + k_d s = \frac{k_d s^2 + k_p s + k_i}{s} \tag{26}$$

$$k_p e + k_i \int e dt + k_d \frac{de}{dt} \tag{27}$$

A control signal is provided to the plant in accordance with the PID controller operating principle in order to achieve a new output value. In order to determine the new error, the new output value will be transmitted back to the sensor once more. The controller will then use this new error as an input signal to determine the gain values for k_p, k_i, and k_d.

2.5. Firefly algorithm

Optimization problems have been extensively studied in various branches of science, requiring the identification of optimal solutions for decision variables through specific algorithms. These optimization algorithms play a crucial role in exploring the search space of a problem to find the most optimal solution [29]. The primary focus of these algorithms is to optimize or minimize the objective function, which may include aspects such as efficiency, revenue, cost, and performance. Consequently, a large number of optimization algorithms are currently utilized by researchers to achieve the desired optimal solution when dealing with complex problems. Some algorithms mimic the behavior of animals in searching for food, using data from previous individuals to create new solutions. Three widely used algorithms are the Artificial Bee Colony (ABC), Particle Swarm Optimization (PSO), and Firefly Algorithm (FA). These algorithms have been widely applied in various applications due to their rapid exploration capabilities and their adaptability to different types of problems [30].

The Firefly Algorithm (FA) is acknowledged as one of the most efficient algorithms, as demonstrated in the research cited in Ref. [31]. It is inspired by the behavior and light intensity of fireflies. Fireflies exhibit varying degrees of brightness due to their ability to produce light through bioluminescence. The purpose of this luminescence is multifaceted, encompassing the attraction of suitable mates, acting as a warning system for safety, and facilitating the capture of prey [30]. The unique frequencies of flashes, which attract male and female fireflies, are determined by the speed and length of the light. The Firefly Algorithm is a metaheuristic algorithm inspired by the flickering behavior of fireflies and is based on swarm dynamics [32]. In this method, a firefly attractiveness is directly related to its luminosity, as determined by the objective function. According to Ref. [33], it is assumed that all fireflies are unisex, meaning any firefly can be attracted to another. The luminosity of a firefly decreases with increasing distance from the observer, in accordance with the law that governs the luminous intensity of fireflies. The firefly attraction function is defined as follows, referring to Eq. (28).

$$\beta(r) = \beta_0 e^{-\gamma r^m}, (m \geq 1) \tag{28}$$

The distance between two fireflies *i* and *j* on x_i and x_j, is the cartesian distance which is formulated as follows, referring to Eq. (29).

$$r_{ij} = \left\| x_i - x_j \right\| = \sqrt{\sum_{k=1}^{d} \left(x_{i,k} - x_{j,k} \right)^2} \tag{29}$$

The difference from firefly to firefly location coordinates is between the two (r_{ij}). The equation for the optimal movement of fireflies that results in light intensity is presented in Eq. (30).

$$x_i = x_i + \beta_0 e^{-\gamma r^2} \left(x_i - x_j \right) + \alpha \left(rand - \frac{1}{2} \right) \tag{30}$$

Research to date indicates that the algorithm tends to exhibit relaxation with constant parameters and is prone to premature convergence. Several academics have modified the algorithm in various ways to enhance its performance [34]. In this study, we have updated the default firefly method to simplify searches using various probability distributions. This was achieved through changes to the parameters, revised search tactics, and adjustments to the solution space, as demonstrated in Table 4.

The process design for the firefly algorithm are as follows:

Step 1. Setting parameters such as number of fireflies, iterations, constants

Step 2. Initialize the specified firefly parameters using the rand. function

Step 3. Evaluate each position, and the level of success for all fireflies using the objective function.

Step 4. Update the position of the brightest fireflies

Step 5. After the fireflies reach the specified minimum value, the next step is to get the k_p, k_i, and k_d values.

Based on the Firefly algorithm parameters presented in Table 4, the

Table 4
Firefly algorithm parameters.

Parameters	Values
Number of fireflies	20
Number of Iteration	50
Alpha (α)	0.9
Betamin (β)	0.5
Gamma (γ)	0.2

following explanations can be provided: The number of fireflies used in this algorithm is 20, aiming to achieve a balance between computational efficiency and accuracy in solution searching. The algorithm is set to run for 50 iterations, which allows adequate time for the algorithm to reach convergence while avoiding excessively long computational processes. As for the alpha (α) value, it is set at 0.9 to encourage extensive exploration within the search space and reduce the risk of becoming trapped in local minima. The Betamin (β) value, set at 0.5, plays a role in influencing the interaction among fireflies, thereby expanding their search coverage. Furthermore, the Gamma (γ) value is set at 0.2 to regulate light absorption, affecting the attraction between fireflies over longer distances. Regarding the convergence process, it is achieved when there is a significant decrease in the change of firefly brightness, and we use an indicator based on the smallest change in brightness value. If this change falls below a certain threshold for 10 consecutive iterations, the algorithm is considered to have converged. Finally, the termination criteria of the algorithm involve stopping after 50 iterations or when the change in PID parameter values reaches a low level, indicating that an optimal solution has been obtained. These criteria, based on empirical testing, ensure that the algorithm does not terminate its process prematurely before finding the most optimal solution.

3. Results and observations

Based on the method that has been proposed, there are some tests that must be conducted. The first is to investigate how PID control affects the DC-DC Boost Converter and BLDC motor. The second is to investigate how the firefly algorithm influences changes in the DC-DC Boost Converter.

3.1. Solar photovoltaic

In simulation and testing for the 200 W Solar Photovoltaic has been modeled based on the electrical characteristics. The *I–V* and *P–V* characteristics which provide information about the operational state of the system are shown in Fig. 8.

Fig. 8 shows the characteristics of the I–V and P–V graphs of a PV module. The current-voltage (I–V) curve illustrates the relationship between the current and the voltage generated by a PV cell, while the power-voltage (P–V) curve depicts the power output of a PV module under various radiation levels and temperatures. Since these characteristics vary with changing environmental conditions, they are important indicators of how efficiently a photovoltaic system can generate electricity from sunlight.

3.2. DC-DC boost converter

Based on the parameter values in Table 2 and the mathematical model equation in Eq. (18), the transfer function for the DC-DC Boost Converter circuit is obtained as follows:

$$\frac{V_{out}}{V_{in}} = \frac{R}{RCLs^2 + Ls + R} \tag{18b}$$

$$\frac{V_{out}}{V_{in}} = \frac{100}{100.4,7.10^{-8}.4,7.10^{-3}s^2 + 4,7.10^{-3}s + 100}$$

$$G(s) = \frac{V_{out}}{V_{in}} = \frac{1}{22.09.10^{-11}s^2 + 4,7.10^{-3}s + 100}$$

Hence, the transfer function equation for the DC-DC Boost Converter circuit is obtained as follows:

$$G(s) = \frac{1}{22.09.10^{-11}s^2 + 4,7.10^{-3}s + 100}$$

3.3. Mathematical model of BLDC motor

Based on Eq. (25) and the parameter values in Table 4, the transfer function of the BLDC motor can be obtained as follows:

$$G(s) = \frac{\omega_m}{V_s} = \frac{{}^{1}/_{K_e}}{\tau_m \tau_e s^2 + \tau_m s + 1} \tag{25b}$$

$$\tau_m = \frac{RJ}{K_e K_t} = \frac{1.835}{0,0521x0,0521} = \frac{1.835}{0,002714} = 6,670.10^3$$

$$\tau_e = \frac{L}{3R} = \frac{2,87.10^2}{3.1,835} = \frac{2,87.10^2}{5,505} = 0,0521.10^2$$

$$G(s) = \frac{\omega_m}{V_s} = \frac{{}^{1}/_{0.0521}}{6,670.10^3 x0,0521.10^2 s^2 + 6,670.10^3 s + 1}$$

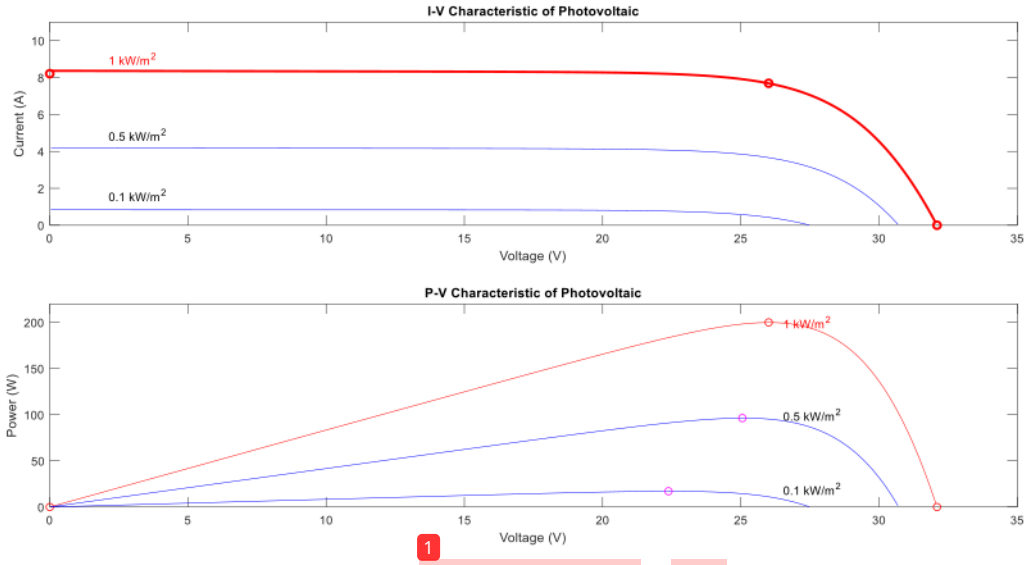

Fig. 8. Graphic *I–V* and *P–V* characteristics of PV module.

$$G(s) = \frac{\omega_m}{V_s} = \frac{19,19386}{0,3475.10^5 s^2 + 6,670.10^3 s + 1}$$

Then the mathematical model of the transfer function equation for the BLDC motor circuit is as follows:

$$G(s) = \frac{19,19386}{0,3475.10^5 s^2 + 6,670.10^3 s + 1}$$

3.4. Optimization DC-DC boost converter of BLDC motor using PID controller

The optimization of the PID controller in the DC-DC Boost Converter is intended to ensure an adequate response to potential disturbances and variations in line and load voltages. The simulation block for testing the optimization of the DC-DC Boost Converter as a BLDC motor drive, using a PID controller, is shown in Fig. 9.

The purpose of tuning the PID controller is to get values for the proportional, integral, and derivative amplifiers of the controller so that the smallest possible error signal value is obtained. The test and simulation results obtained for the PID controller parameters were P = 101.44808, I = 0.08456, and a value of D is −292.72358, with a graph of the simulation results shown in Fig. 10.

Fig. 10 shows that optimization using the PID controller in the DC-DC Boost Converter circuit results in an overshoot performance at the start of the start of 11.4 % and the rise time value is 499 s. This is due to the absence of precise parameter values for k_p, k_i, and k_d values. So it is necessary to improve the system response in the DC-DC Boost Converter circuit. The overall performance of the DC-DC Boost Converter circuit performance indicators is shown in Table 5. Besides that, Fig. 10 shows the results of Optimizing the DC-DC Boost Converter Using a PID Controller showing the desired results. PID controllers have proven to be a reliable and effective solution for controlling the output voltage of DC-DC Boost Converters. This optimization process provides an efficient way to achieve the desired output voltage with greater accuracy. It is also advantageous in terms of cost and energy efficiency compared to other control techniques. All in all, the PID controller is a great choice to optimize the DC-DC Boost Converter to get the best output.

3.5. Optimization DC-DC boost converter of BLDC motor using PID controller and firefly algorithm

The next testing stage is the DC-DC Boost Converter which is optimized using a PID controller tuned with the firefly algorithm. The test results for simulating the optimization of the PID controller with the firefly algorithm on the DC-DC Boost Converter circuit as a BLDC motor drive are shown in Fig. 11.

The optimization results using the firefly algorithm on the PID controller system obtained parameter values for each PID parameter, namely $k_p = 97.7668$, $k_i = 0.0091$, and $k_d = -0.1270$. The optimization results obtained and performance values are shown in Table 6. In addition, the graph shows that the optimization results of the DC-DC Boost Converter with the PID controller used in combination with the firefly algorithm can achieve maximum efficiency. The PID controller functions to set the parameters of the firefly algorithm to ensure that the optimization process is converged quickly and accurately. This makes the PID-Firefly algorithm an ideal choice for optimizing DC-DC Boost Converter systems as it offers a balance between speed and accuracy.

The transient response performance indicator for optimizing DC-DC Boost Converter circuit as a BLDC motor drive using the PID-Firefly algorithm shows that the rise time value has increased by 820 s while the settling time value has decreased to 2.07e+03 s. The overshoot value becomes 0 % which was previously 11.4 %.

3.6. The advantages of the firefly algorithm in optimizing the DC-DC boost converter

The utilization of the Firefly algorithm in the optimization of Boost Converter systems employed for Brushless DC (BLDC) motor drives, particularly in conjunction with Proportional-Integral-Derivative (PID) control, has notable benefits. The utilization of the Firefly Algorithm in comparison to conventional PID control has been observed to yield significant disparities, as illustrated in Fig. 12, through comparative testing and simulations.

The rise time has increased from 499 s to 820 s, indicating a slower initial response with the implementation of the Firefly Algorithm. However, a significant reduction in settling time is observed, decreasing from 3.33 e+03 s to 2.07 e+03 s. Additionally, there is a notable decrease in the overshoot value from 11.4 % to zero, signifying a substantial improvement in performance. This observation suggests that while the Firefly Algorithm initially exhibits a delayed reaction, it effectively achieves a stable state more quickly and efficiently, while also ensuring that the desired voltage threshold is not exceeded. The use of the firefly algorithm methodology, despite its initial slowness, appears to facilitate the attainment of stability without excessive deviation, thereby enhancing the overall efficiency of the system.

4. Conclusions

The results of the planning and design optimization of the DC-DC Boost Converter circuit as a BLDC motor drive using a PID controller optimized with the firefly algorithm can be concluded as follows:

1. The findings from our research suggest that the efficiency of the BLDC motor can be improved by implementing a PID controller that has been developed using the firefly algorithm. The rise time of the BLDC motor improved by 64.33 %, increasing from an initial value of 499 s–820 s.
2. The optimization method has reduced the settling time of the system from 3.33 e+03 s to 2.07 e+03 s. This drop indicates an improvement in the system reaction, which may be measured as an increase in the system speed in achieving stability after disruptions. The increase of 37.77 % indicates a decrease in the time needed for the system to reach a stable state following optimization.
3. The installation of the firefly algorithm has effectively decreased the overshoot from 11.4 % to 0 %. This signifies that the system has

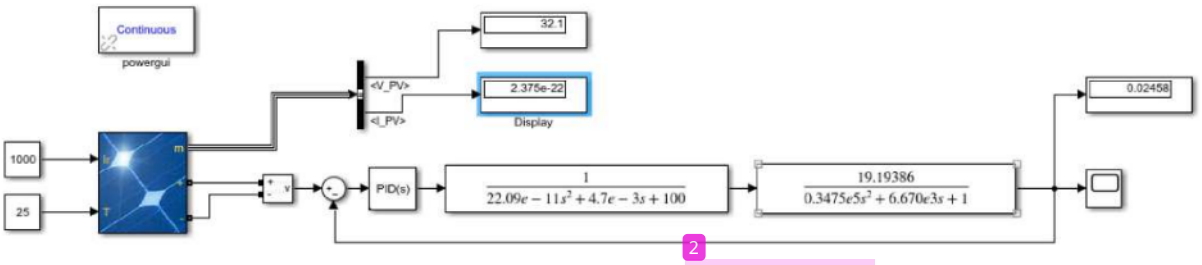

Fig. 9. Simulink block diagram for optimization of DC-DC boost converter.

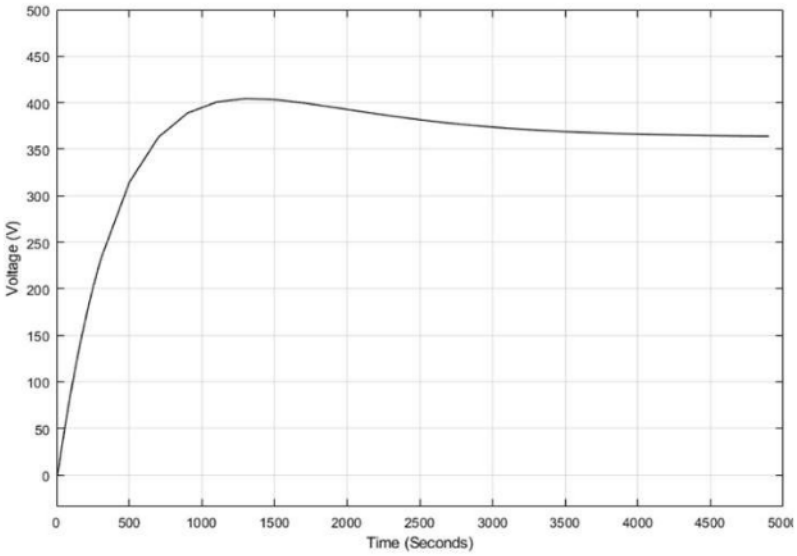

Fig. 10. Results of optimizing the DC-DC boost converter using a PID controller.

Table 5
Transient Response Test Results with the PID controller.

System Performance Parameters	Value
RiseTime	499 s
SettlingTime	3.33 e+03 s
Overshoot	11.4 %
Peak	1.11

attained an elevated degree of control subsequent to optimization. Put simply, the system has gotten more prompt and proficient at obtaining the desired value without surpassing it, indicating a notable enhancement in system control.

CRediT authorship contribution statement

Izza Anshory: Conceptualization, Data curation, Formal analysis, Funding acquisition, Methodology, Project administration, Writing - original draft. **Jamaaluddin Jamaaluddin:** Data curation, Visualization. **Arief Wisaksono:** Project administration, Resources. **Indah Sulistiyowati:** Investigation, Validation. **Hindarto:** Formal analysis,

Table 6
Transient response test results with PID -firefly algorithm.

System Performance Parameters	Values
RiseTime	820 s
SettlingTime	2.07 e+03 s
Overshoot	0 %
Peak	0.993

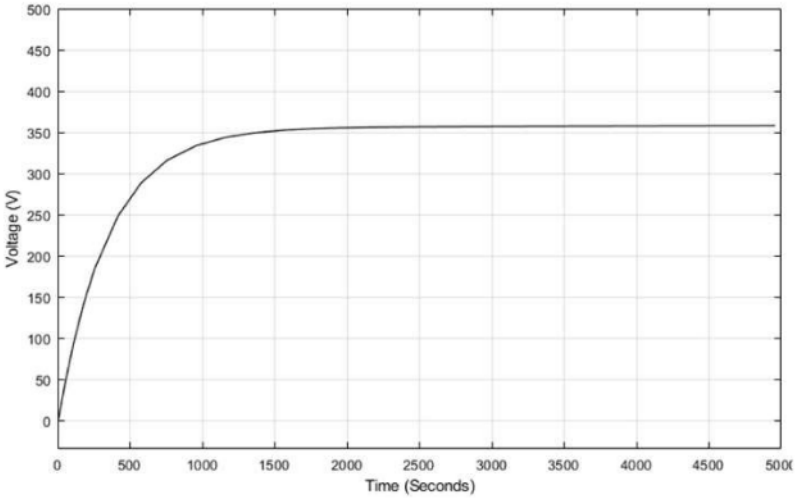

Fig. 11. Results of optimization DC-DC boost converter using a PID-Firefly algorithm.

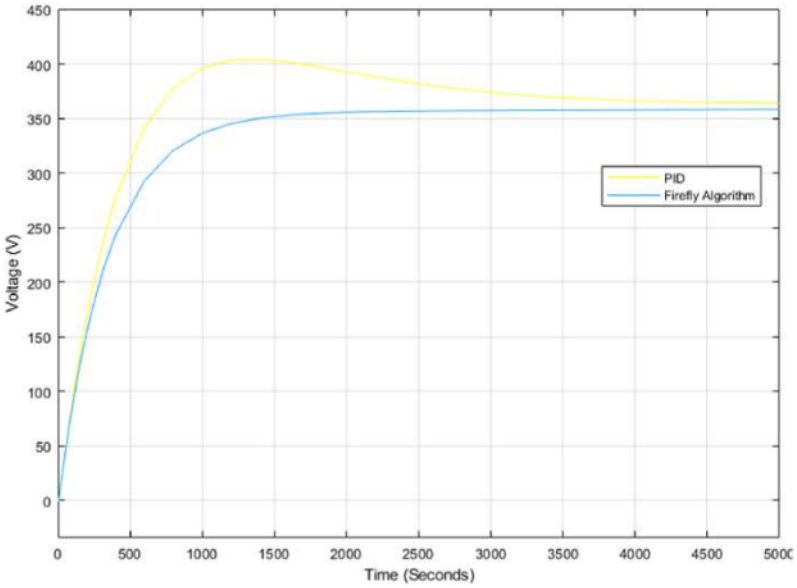

Fig. 12. Comparison of PID control optimization and firefly algorithm.

Funding acquisition, Software. **Bagus Setya Rintyarna:** Investigation, Validation. **Ahmad Fudholi:** Supervision, Writing - original draft, Writing - review & editing. **Yuli Asmi Rahman:** Formal analysis, Visualization. **Kamaruzzaman Sopian:** Resources, Supervision.

Declaration of competing interest

The authors declare that they have no known competing financial interests or personal relationships that could have appeared to influence the work reported in this paper.

Data availability

Data will be made available on request.

Acknowledgements

Authors grateful to The Directorate of Research and Community Service (DRPM) Universitas Muhammadiyah Sidoarjo and Research Center for Energy Conversion and Conservation, National Research and Innovation Agency (BRIN), Indonesia for providing financial assistance for research activities.

Nomenclature

ABC	Artificial Bee Colony
ANN	Artificial Neural Network
BLDC	Brushless Direct Current
CO_2	Carbon dioxide
CS	Cuckoo Search
DC-DC	Direct Current – Direct Current
EMF	Electromotive force
FA	Firefly Algorithm
FOPID	Fractional Order PID
FFOPID	Fractional Order Fuzzy PID controller
GA	Genetic Algorithm
IC	Incremental Conductance
LQR	Linear Quadratic Regulator
MPC	Model Predictive Control
MPP	Maximum Power Point
MPPT	Maximum Power Point Tracking
PID	Proportional Integral Derivative
PWM	Pulse Widht Modulation
PV	Photovoltaic
PSO	Particle Swarm Optimization
SMPS	Switched-Mode Power Supply
SPV	Solar Photo Voltaic
THD	Total Harmonic Distortion
VSI	Voltage Source Inverter

References

[1] M. Abdillah, R.C. Batubara, N.I. Pertiwi, H. Setiadi, Design of maximum power point tracking system based on single Ended primary inductor converter using Fuzzy Logic controller, International Journal of Intelligent Engineering and Systems 15 (1) (2022) 350–360, https://doi.org/10.22266/IJIES2022.0228.32.

[2] V. kumar, R. kumar Bindal, A comparative analysis of effective MPPT technology for photovoltaic system with boost converter, Mater. Today Proc. 69 (2022), https://doi.org/10.1016/j.matpr.2022.11.026. A1–A5.

[3] A.M. Gabor, et al., The impact of cracked solar cells on solar panel energy delivery, in: Conference Record of the IEEE Photovoltaic Specialists Conference, 2020-June, 2020, p. 810, https://doi.org/10.1109/PVSC45281.2020.9300743. –0813.

[4] A. Cordeiro, V. Fernão Pires, D. Foito, A.J. Pires, J.F. Martins, Three-level quadratic boost DC-DC converter associated to a SRM drive for water pumping photovoltaic powered systems, Sol. Energy 209 (Oct. 2020) 42–56, https://doi.org/10.1016/j.solener.2020.08.076.

[5] R. Kumar, B. Singh, Solar PV powered-sensorless BLDC motor driven water pump, IET Renew. Power Gener. 13 (3) (Feb. 2019) 389–398, https://doi.org/10.1049/iet-rpg.2018.5717.

[6] P. Srivastava, V.K. Tiwari, Speed control of BLDC motor fed from solar pv array using particle swarm optimization. Proceedings of the 2020 9th International Conference on System Modeling and Advancement in Research Trends, SMART, 2020, pp. 392–397, https://doi.org/10.1109/SMART50582.2020.9337111, 2020.

[7] D.S. Rani, M. Muralidhar, BLDC motor driven for solar Photo voltaic powered air cooling system, Int. J. Energy Power Eng. 11 (9) (2018) 1049–1056.

[8] M. Farhadi-Kangarlu, M.G. Marangalu, "Five-Level single-DC source inverter with adjustable DC-link voltage," *26th Iranian Conference on electrical engineering*, ICEE (2018) 1017–1021, https://doi.org/10.1109/ICEE.2018.8472625, 2018.

[9] A. Vazani, et al., Composite nonlinear feedback control of a DC-DC boost converter under input voltage and load variation, Int. J. Electr. Power Energy Syst. 155 (Jan) (2024), https://doi.org/10.1016/j.ijepes.2023.109562.

[10] C.O. Omeje, A.O. Salau, Torque ripples enhancement of a PMBLDC motor propelled through quadratic DC–DC boost converter at varying load, ISA Trans. (2023), https://doi.org/10.1016/j.isatra.2023.08.027.

[11] M.I. Mosaad, M. Osama abed el-Raouf, M.A. Al-Ahmar, F.A. Banakher, Maximum power point tracking of PV system based cuckoo search algorithm; review and comparison, in: Energy Procedia, Elsevier Ltd, 2019, pp. 117–126, https://doi.org/10.1016/j.egypro.2019.04.013.

[12] L.F. da S, C. Pereira, E. Batista, M.A.G. de Brito, R.B. Godoy, A Robustness analysis of a Fuzzy fractional order PID controller based on genetic algorithm for a DC-DC boost converter, Electronics (Switzerland) 11 (12) (2022), https://doi.org/10.3390/electronics11121894.

[13] R. Kumar, B. Singh, Solar photovoltaic array fed canonical switching cell converter based BLDC motor drive for water pumping system, 11th IEEE India Conference: Emerging Trends and Innovation in Technology, INDICON (2014), https://doi.org/10.1109/INDICON.2014.7030454, 2015.

[14] M.A. Islam, A. Merabet, R. Beguenane, H. Ibrahim, "Modeling solar photovoltaic cell and simulated performance analysis of a 250W PV module," *2013 IEEE Electrical Power and Energy Conference*, EPEC (2013) 1–6, https://doi.org/10.1109/EPEC.2013.6802959, 2013.

[15] E.V. Platonova, A.S. Toropov, A.N. Tulikov, Simulation of energy input to solar panels. Proceedings - 2019 International Ural Conference on Electrical Power Engineering, UralCon, 2019, pp. 133–137, https://doi.org/10.1109/URALCON.2019.8877633, 2019.

[16] K. Rajkumar, K.A. Kumar, Application of firefly algorithm for power estimations of solar photovoltaic power plants, Energy Sources, Part A Recovery, Util. Environ. Eff. 00 (00) (2021) 1–16, https://doi.org/10.1080/15567036.2021.1916653.

[17] M. Belarbi, K. Haddouche, B. Sahli, E.H. Belarbi, A. Boudghene-Stambouli, B. Khiali, Self-reconfiguring MPPT to Avoid Buck-Converter Limits in Solar Photovoltaic Systems," *Renewable and Sustainable Energy Reviews*, vol. 82, Elsevier Ltd, 2018, pp. 187–193, https://doi.org/10.1016/j.rser.2017.09.019.

[18] C.R. Algarín, A.O. Castro, J.C. Naranjo, Dual-axis solar tracker for using in photovoltaic systems, International Journal of Renewable Energy Research 7 (1) (2017) 137–145, https://doi.org/10.20508/ijrer.v7i1.5147.g6973.

[19] S.Y. Chen, B.C. Yang, T.A. Pu, C.H. Chang, R.C. Lin, Active current sharing of a parallel DC-DC converters system using bat algorithm optimized two-DOF PID control, IEEE Access 7 (2019) 84757–84769, https://doi.org/10.1109/ACCESS.2019.2925064.

[20] J. Jumiyatun, M. Mustofa, Controlling DC-DC Buck converter using Fuzzy-PID with DC motor load, IOP Conf. Ser. Earth Environ. Sci. 156 (1) (2018), https://doi.org/10.1088/1755-1315/156/1/012003.

[21] R. Kumar, S. Member, BLDC Motor Driven Water Pump Fed by Solar Photovoltaic Array Using Boost Converter (2015) 2–7.

[22] B. Achiammal, "Design of PID controller for boost converter using particle swarm optimization, Algorithm 1 (4) (2017) 72–76.

[23] L. Ardhenta, R.K. Subroto, "Application of direct, MRAC in PI controller for DC-DC boost converter 11 (2) (2020) 851–858, https://doi.org/10.11591/ijpeds.v11.i2.pp851-858.

[24] M. Ridwan, M.N. Yuniarto, Soedibyo, Electrical Equivalent Circuit Based Modeling and Analysis of Brushless Direct Current (BLDC) Motor," *Proceeding - 2016 International Seminar on Intelligent Technology and its Application, ISITIA 2016: Recent Trends in Intelligent Computational Technologies for Sustainable Energy*, 2017, pp. 471–478, https://doi.org/10.1109/ISITIA.2016.7828706.

[25] M. Archana, J.A. Thulasi, M.B.J. Ananth, "An efficient solar power based four quadrant operation of BLDC motor," *International Conference on Electrical, Electronics, and Optimization Techniques*, ICEEOT (2016) 4841–4846, https://doi.org/10.1109/ICEEOT.2016.7755640, 2016.

[26] R. Anand, S. Saravanan, "Solar PV system for energy Conservation incorporating an MPPT based on computational intelligent techniques supplying brushless DC motor drive,", June (2016) https://doi.org/10.4236/cs.2016.78142.

[27] S. Bharat, A. Ganguly, R. Chatterjee, S. Member, B. Basak, D. Sheet, A review on tuning methods for PID controller, Asian Journal of Convergence in Technology V (I) (2019) 1–4.

[28] M.A. Ibrahim, A.K. Mahmood, N.S. Sultan, Optimal PID controller of a brushless DC motor using genetic algorithm, Int. J. Power Electron. Drive Syst. 10 (2) (2019) 822–830, https://doi.org/10.11591/ijpeds.v10.i2.822-830.

[29] Z. Cheng, H. Song, D. Zheng, M. Zhou, K. Sun, Hybrid firefly algorithm with a new mechanism of gender distinguishing for global optimization, Expert Syst. Appl. (Aug) (2023) 224, https://doi.org/10.1016/j.eswa.2023.120027.

[30] M. Ghasemi, S. kadkhoda Mohammadi, M. Zare, S. Mirjalili, M. Gil, R. Hemmati, A new firefly algorithm with improved global exploration and convergence with application to engineering optimization, Decision Analytics Journal 5 (Dec) (2022), https://doi.org/10.1016/j.dajour.2022.100125.

[31] I. Anshory, I. Robandi, J. Jamaaluddi, A. Fudholi, Wirawan, Transfer function modeling and optimization speed response of bldc motor e-bike using intelligent controller, J. Eng. Sci. Technol. (2021).

[32] X. Zhang, S. Wang, Firefly search algorithm based on leader strategy, Eng. Appl. Artif. Intell. (Aug) (2023) 123, https://doi.org/10.1016/j.engappai.2023.106328.

[33] H. Setiadi, K.O. Jones, Power system design using firefly algorithm for dynamic stability enhancement, Indonesian Journal of Electrical Engineering and Computer Science 1 (3) (2016) 446–455, https://doi.org/10.11591/ijeecs.v1.i3.pp446-455.

[34] S. Bazi, R. Benzid, Y. Bazi, M.M. Al Rahhal, A fast firefly algorithm for function optimization: application to the control of bldc motor, Sensors 21 (16) (2021), https://doi.org/10.3390/s21165267.

sktp-19-04-2024 07_06_36-21432

ORIGINALITY REPORT

4%	2%	8%	0%
SIMILARITY INDEX	INTERNET SOURCES	PUBLICATIONS	STUDENT PAPERS

PRIMARY SOURCES

1	"Renewable Power for Sustainable Growth", Springer Science and Business Media LLC, 2021 Publication	2%
2	Darmansyah Darmansyah, Imam Robandi. "Intelligent voltage controller based on firefly algorithm for DC-DC boost converter", Indonesian Journal of Electrical Engineering and Computer Science, 2022 Publication	2%

Exclude quotes	On	Exclude matches	< 2%
Exclude bibliography	On		